Diabetologia (2012) 55:1195–1204
DOI 10.1007/s00125-011-2428-6

ARTICLE

Mice expressing a human K_{ATP} channel mutation have altered channel ATP sensitivity but no cardiac abnormalities

R. Clark · R. Männikkö · D. J. Stuckey · M. Iberl · K. Clarke · F. M. Ashcroft

Received: 6 June 2011 / Accepted: 28 November 2011 / Published online: 18 January 2012

Abstract
Aims/hypothesis Patients with severe gain-of-function mutations in the Kir6.2 subunit of the ATP-sensitive potassium (K_{ATP}) channel, have neonatal diabetes, muscle hypotonia and mental and motor developmental delay—a condition known as iDEND syndrome. However, despite the fact that Kir6.2 forms the pore of the cardiac K_{ATP} channel, patients show no obvious cardiac symptoms. The aim of this project was to use a mouse model of iDEND syndrome to determine whether iDEND mutations affect cardiac function and cardiac K_{ATP} channel ATP sensitivity.
Methods We performed patch-clamp and in vivo cine-MRI studies on mice in which the most common iDEND mutation (Kir6.2-V59M) was targeted to cardiac muscle using Cre-lox technology (m-V59M mice).
Results Patch-clamp studies of isolated cardiac myocytes revealed a markedly reduced K_{ATP} channel sensitivity to MgATP inhibition in m-V59M mice (IC_{50} 62 μmol/l compared with 13 μmol/l for littermate controls). In vivo cine-MRI revealed there were no gross morphological differences and no differences in heart rate, end diastolic volume, end systolic volume, stroke volume, ejection fraction, cardiac output or wall thickening between m-V59M and control hearts, either under resting conditions or under dobutamine stress.
Conclusions/interpretation The common iDEND mutation Kir6.2-V59M decreases ATP block of cardiac K_{ATP} channels but was without obvious effect on heart function, suggesting that metabolic changes fail to open the mutated channel to an extent that affects function (at least in the absence of ischaemia). This may have implications for the choice of sulfonylurea used to treat neonatal diabetes.

Keywords ATP-sensitive potassium channel · Cardiac ischaemia · MRI · Kir6.2 · Sulfonylurea receptor

Abbreviations

FLASH	Fast low-angle-shot
FRT	FLP recombinase target
GFP	Green fluorescent protein
iDEND	Intermediate DEND syndrome
IRES	Internal ribosome entry site
K_{ATP} channel	ATP-sensitive potassium channel
LV	Left ventricle
Mck-Cre mice	Mice expressing Cre recombinase under the control of the muscle creatine kinase promoter
m-V59M mice	Mice carrying Kir6.2-V59M subunits in heart and skeletal muscle tissue

R. Clark, R. Männikkö and D. J. Stuckey contributed equally to this study.

R. Clark · R. Männikkö · D. J. Stuckey · M. Iberl · K. Clarke · F. M. Ashcroft (✉)
Henry Wellcome Centre for Gene Function,
Department of Physiology, Anatomy and Genetics,
Parks Road,
Oxford OX1 3PT, UK
e-mail: frances.ashcroft@dpag.ox.ac.uk

R. Clark · R. Männikkö · M. Iberl · K. Clarke · F. M. Ashcroft
OXION, University of Oxford,
Oxford, UK

Present address:
R. Männikkö
Molecular Neuroscience, Institute of Neurology, UCL,
London, UK

Present address:
D. J. Stuckey
Biological Imaging Centre, National Heart and Lung Institute,
Imperial College, Hammersmith Hospital,
London, UK

MRI	Magnetic resonance imaging
SUR	Sulfonylurea receptor
WT	Wild-type

Introduction

Gain-of-function mutations in either *KCNJ11* or *ABCC8*, which encode the pore-forming (Kir6.2) and regulatory (SUR1) subunits of the ATP-sensitive potassium (K_{ATP}) channel, are a common cause of neonatal diabetes, a rare inherited disorder characterised by the development of diabetes within the first 6 months of life [1–5]. In addition to diabetes, about 20% of patients experience neurological problems, such as motor and mental developmental delay, and muscle hypotonia, a condition now known as intermediate DEND (iDEND) syndrome [3, 6]. A very few (<3%) also suffer from epilepsy.

This diverse spectrum of symptoms arises because K_{ATP} channels are present in multiple tissues, where they play important physiological roles by coupling cell metabolism to the electrical excitability of the plasma membrane [5, 7–9]. Metabolically induced changes in channel activity are produced by altered intracellular adenine nucleotide concentrations, with ATP inhibiting and MgADP (and MgATP) stimulating channel activity [9–12]. All K_{ATP} channel mutations causing neonatal diabetes examined to date impair the ability of MgATP to close the channel, thereby suppressing electrical excitability and cell function. In pancreatic beta cells, for example, K_{ATP} channels link changes in blood glucose concentration to insulin secretion [13]. When blood glucose, and thus beta cell metabolism, are low K_{ATP} channels are open. This maintains the membrane potential at a hyperpolarised level and dampens down electrical activity, switching off insulin secretion. An increase in metabolic activity closes K_{ATP} channels, depolarising the beta cell and increasing electrical activity and insulin release. Neonatal diabetes results when mutant K_{ATP} channels fail to close in response to elevation of blood glucose [2–5, 14, 15].

K_{ATP} channels also influence the electrical excitability of many different types of neuron, and impaired neuronal electrical activity likely underlies the neurological phenotype of iDEND patients. Indeed, recent studies suggest that the muscle hypotonia found in iDEND patients is also a consequence of the presence of mutant K_{ATP} channels in neuronal tissue [16].

As in endocrine and neuronal cells, Kir6.2 serves as the pore-forming subunit of cardiac K_{ATP} channels, raising the possibility that gain-of-function mutations in *KCNJ11* might affect cardiac function. Both the sulfonylurea receptors SUR1 and SUR2A (encoded by *ABCC8* and *ABCC9*, respectively) are present in the heart, and pharmacological studies and studies of knockout animals suggest that Kir6.2/SUR2A forms the ventricular K_{ATP} channel [17–19] and Kir6.2/SUR1 the atrial K_{ATP} channel [20]. Despite the fact that K_{ATP} channels were first identified in cardiac myocytes [21], where they are found at high density, their functional role in the heart is less well understood than in other tissues [7]. Under normal conditions, ventricular K_{ATP} channels appear to be closed and do not contribute to the normal excitability of the heart. Instead, they are thought to play a protective role during severe metabolic stress, when opening of K_{ATP} channels leads to action potential shortening and contractile failure, thereby conserving cellular ATP levels [22]. Compelling evidence of the importance of KIR6.2/SUR2A channels in cardiac stress comes from studies of knockout mice (*Kcnj11*$^{-/-}$ and *Sur2*$^{-/-}$) where action potential shortening in response to anoxia is absent, and both ischaemic and pharmacological preconditioning are not observed [19, 23]. Mice lacking K_{ATP} channels also show abnormal vulnerability to a variety of other physiological and pathological stresses including sympathetic surge [24, 25], physical exertion [26], mineralocorticoid-induced hypertension [27] and volume and pressure overload [26, 28]. In atrial cells, Kir6.2/SUR1 channels may potentially contribute to the control of action potential frequency and heart rate.

These data therefore raise the question of whether gain-of-function mutations in *KCNJ11* that cause human neonatal diabetes might affect cardiac function: for example, by affecting heart rate or increasing stress tolerance. Indeed, pharmacological activation of K_{ATP} channels with pinacidil enhanced arrhythmogenicity in tissue isolated from human hearts [29]. Strikingly, a transgenic mouse selectively overexpressing two Kir6.2 gain-of-function mutations (an N-terminal deletion of 30 amino acids and a K185Q point mutation; ΔN30,K185Q mice) in the heart showed no gross physiological or morphological cardiac problems [30, 31]. Electrocardiograms were normal, although there was a slight reduction in the mean 24 h heart rate. Unexpectedly, isolated myocyte experiments revealed that, despite a 40-fold reduction in ATP sensitivity, the channel remained largely closed in intact cells and action potential duration was unaffected [31]. This was in marked contrast to the effects of a similar transgene expressed in pancreatic beta cells, which produced a severe diabetic phenotype [15]. However, in contrast to hearts from control animals, β-adrenergic stimulation did not cause a positive ionotropic response in isolated, perfused transgenic hearts, and transgenic hearts also exhibited a higher left ventricular developed pressure under resting conditions [32].

The extent to which these mice mimic the phenotype of human neonatal diabetes is, however, unclear. All patients with neonatal diabetes caused by *KCNJ11* mutations are heterozygotes and increased K_{ATP} channel density is not expected, whereas the transgenic mice strongly overexpress

Kir6.2-ΔN30,K185Q and are expected to have homozygous mutant K_{ATP} channels. In addition, as the transgene was not targeted to a specific location in the genome, it might have disrupted an endogenous gene. Further, most studies of these mice were conducted ex vivo using isolated, perfused hearts and studies of in vivo cardiac function were limited. To date, there have been no reports of cardiac abnormalities in neonatal diabetes patients, but it is unclear whether the effects of cardiac stress have been examined. In this paper, we therefore explore the effect that a human mutation causing neonatal diabetes (Kir6.2-V59M) has on the in vivo function of the heart. We chose this mutation as it is the most common mutation causing iDEND syndrome [3].

Methods

Generation of m-V59M mice

Mice expressing Kir6.2-V59M in heart and skeletal muscle tissue (m-V59M mice) were generated using a Cre-lox approach. The *Kcnj11* gene encoding a mutant Kir6.2-V59M subunit, preceded by a loxP-flanked STOP sequence and followed by an FRT-flanked internal ribosome entry site followed by a GFP cassette, was targeted to the ROSA26 locus to ensure that a single copy of the mutant gene was expressed from a known location [14]. The endogenous ROSA promoter was used to prevent excess gene expression. To generate mice that express the transgene specifically in muscle tissue, ROSA26StopKir6.2-V59M$^{lox/+}$ mice (ROSA mice) were crossed with mice expressing Cre recombinase under the control of the muscle creatine kinase promoter (Mck-Cre mice) [33]. The latter were kindly provided by J. Brüning (Institute of Genetics, Cologne, Germany). This generated mice (m-V59M mice) in which expression of Cre recombinase in heart and skeletal muscle leads to deletion of the STOP cassette and thus to expression of the mutant gene encoding Kir6.2-V59M [14]. Wild-type (WT), Mck-Cre and ROSA littermates were used as controls. All experiments were carried out on 12-week-old mice.

Animal care

All experiments were conducted in accordance with the UK Animals Scientific Procedures Act (1986) and University of Oxford ethical guidelines. Mice were housed in same-sex littermate groups of two to eight, in a temperature- and humidity-controlled room on a 12 h light/dark cycle (lights on at 06:00 hours). Regular chow food (Teklad Global 2019; Harlan Teklad Global Diet, Blackthorn, UK) containing 55% carbohydrate, 19% protein and 9% fat was freely available. Mice had ad libitum access to water at all times. Genotypes were identified by PCR using genomic DNA isolated from ear biopsies, as previously described [16].

Molecular biology

RNA extraction and cDNA synthesis Muscle and brain tissues were isolated from m-V59M and control mice, immersed in RNALater solution (Qiagen, Crawley, UK), kept at 4°C for 1 h and thereafter stored at −80°C until ready to process. Total RNA was extracted from 30 mg of tissue using an RNeasy Mini Kit (Qiagen), including an on-column DNase digestion step to remove traces of genomic DNA. RNA concentration was determined using a NanoDrop ND-1000 spectrophotometer (Thermo Scientific, Wilmington, USA), and its integrity verified with an Agilent Bioanalyzer (Agilent, South Queensferry, UK). Total RNA, 1 μg, was reverse transcribed in a 20 μl final volume using the High Capacity cDNA Reverse Transcription kit (Applied Biosystems, Warrington, UK). Another sample of total RNA, 1 μg, was processed identically, but with no reverse transcriptase present (non-RT control).

Semi-quantitative PCR Mouse *Kcnj11* transcript was amplified by PCR using cDNA prepared from muscle and brain tissues from m-V59M and control mice, as previously described [16]. PCR products were digested with BtsCI (New England Biolabs, Hitchin, UK) for ~2 h at 50°C. Digested PCR fragments were visualised on an agarose gel with ethidium bromide.

Quantitative RT-PCR All cDNA samples were diluted to 4 ng/μl with nuclease-free water (Sigma Aldrich, Poole, UK). Each reaction consisted of 5 μl (20 ng) cDNA, 12.5 μl 2*PowerSYBR Green I Master Mix (Applied Biosystems), 0.75 μl of 10 μmol/l forward and reverse primers (300 nmol/l) and 6 μl nuclease-free water (total reaction volume 25 μl). Primers for *Kcnj11*, *Abcc9* and reference genes (*Actb*, *Hprt1* and *Hspa8*) were designed and selected as previously described [16]. The primers for *Gfp* were: forward, CGGCGACGTAAACGGCCACA; reverse CAGCTTGCCGGTGGTGCAGA. Reactions were run on an ABI PRISM 7000 sequence detection system (Applied Biosystems). The reaction cycle comprised an initial denaturation for 10 min at 95°C, followed by 40 cycles of 95°C/15 s; 60°C/60 s. All DNA samples were run in triplicate. Non-RT controls were included in each experiment to confirm the absence of genomic DNA contamination.

The 7000 System SDS Software (Applied Biosystems) was used to acquire and analyse PCR data and derive cycle threshold (C_t) values. The ΔC_t method was used to transform C_t values into relative quantities and the highest expression for each primer pair was set to one. The geNorm software was used on the three reference genes to calculate normalisation factors for each tissue. The relative expression

levels of *Kcnj11* and *Abcc9* mRNAs were calculated using this normalisation factor.

K_{ATP} channel recordings from cardiac muscle fibres Mice were killed by cervical dislocation. The heart was immediately removed into Tyrode solution containing (in mmol/l) NaCl 140, KCl 5.4, $CaCl_2$ 1.8, $MgCl_2$ 1, glucose 11, HEPES 5 (pH 7.4) and 10 U/l heparin. The aorta was cannulated and the heart was perfused in a Langerdorf-type apparatus with perfusion buffer containing (in mmol/l) NaCl 120.4, KCl 14.7, KH_2PO_4 0.6, Na_2HPO_4 0.6, $MgSO_4$ 1.2, $NaHCO_3$ 4.6, taurine 30, 2,3-butanedione monoxime 10, glucose 5.5, and HEPES 10 (pH 7.0), for 4 min at a flow rate of 4 ml/min. Ca^{2+}-free collagenase solution (2.4 mg/ml collagenase II [Worthington, Cambridge Biosciences, Cambridge, UK] in perfusion buffer) was perfused for 3–4 min, and then low-Ca^{2+} collagenase solution (40 μmol/l Ca^{2+} in Ca^{2+}-free collagenase solution) for 5–10 min.

The heart was then removed and cut into small pieces in myocyte stopping buffer (10% calf serum and 12.5 μmol/l $CaCl_2$ in perfusion buffer). Cells were further dissociated by gentle pipetting. Ca^{2+} was re-introduced to myocytes by incubating, spinning down, and re-suspending the cells in myocyte stopping buffer with increasing concentrations of $CaCl_2$ added. Myocytes were plated on poly-L-lysine-coated coverslips in high-K^+ Tyrode solution (20 mmol/l K-Tyrode solution, in which 14.6 mmol/l NaCl was replaced by KCl).

K_{ATP} channel activity was recorded in inside-out membrane patches excised from rod-shaped, Ca^{2+}-tolerant cells using an EPC7 amplifier (List Electronik) at a constant holding potential of –60 mV. The pipette solution contained (in mmol/l): 140 KCl, 1.2 $MgCl_2$, 2. $CaCl_2$, 10 HEPES, pH 7.4. The intracellular solution contained (in mmol/l): 155 KCl, 11 EGTA, 2 $MgCl_2$, 1 $CaCl_2$, 10 HEPES, pH 7.2, with MgATP as indicated. To control for possible rundown or reactivation by MgATP, I_c was taken as the mean of the current in control solution (I) before and after ATP application. Concentration–response curves were fitted with a modified Hill equation:

$$I/I_c = 1/\left(1 + \left\{[\mathrm{MgATP}]/\mathrm{IC}_{50}{}^{h}\right\}\right)$$

where [MgATP] is the concentration of MgATP and h is the slope factor.

Cardiac MRI

Cardiac cine-MRI was performed as described [34–36]. Briefly, 12-week-old control and m-V59M mice were anaesthetised with 1.5% isoflurane in O_2 and positioned supine in a purpose-built cradle. ECG electrodes were inserted into the forepaws and a respiration loop was taped across the chest. The cradle was lowered into a vertical-bore, 11.7 T MR system (Magnex Scientific, Oxford, UK) with a 40 mm birdcage coil (Rapid Biomedical, Würzburg, Germany) and a Bruker console running Paravision 2.1.1 (Bruker Medical, Ettlingen, Germany). A stack of contiguous 1 mm thick true short-axis ECG and respiration-gated cine-FLASH images (TE/TR 1.43/4.6 ms; 17.5° pulse; field of view 25.6×25.6 mm; matrix size 256×256; voxel size 100×100×1000 μm; 20–30 frames per cardiac cycle) were acquired to cover the entire left ventricles. Long-axis two- and four-chamber images were also acquired. Image analysis was performed using ImageJ (NIH Image, Bethesda, MD, USA). Left ventricular mass, volumes and ejection fractions were calculated as described [35, 36]. Wall thickness was measured at end diastole and end systole in the interventricular septum and the left ventricular (LV) free wall in a mid LV slice.

Dobutamine stress MRI An intraperitoneal injection of 1.5 mg/kg of dobutamine was performed while mice were still positioned in the scanner, as described by Song et al. [37]. The heart rate typically increased within 2 min of the injection, stabilised at 5 min and remained elevated for over 20 min. Once the heart rate had stabilised, three representative cine-FLASH MR images (basal, mid LV and apical) were acquired at the same locations as were used before dobutamine exposure. Changes in volumes and ejection fraction are reported as the sum of these three slices. The entire in vivo imaging protocol was performed in approximately 50 min. There were no obvious differences observed between the three types of control mouse (WT, ROSA and Mck-Cre) so the data were pooled.

Statistics

Data are expressed as mean±SEM. All n values refer to the number of mice tested. Data were analysed using a repeated-measures ANOVA (with genotype as a between-subject factor and dobutamine treatment as a within-subject factor). Differences were considered significant at $p<0.05$. Statistics were performed using SPSS (IBM, Chicago, IL, USA).

Results

We used a Cre-lox approach in combination with the muscle creatine kinase promoter (Mck-Cre) to selectively target the Kir6.2-V59M mutant subunit to cardiac and skeletal muscle [16]. This avoids any confounding effects due to the high blood glucose concentration and severe diabetes observed when Kir6.2-V59M is targeted to pancreatic beta cells [14].

The expression pattern of WT and mutant *Kcnj11* mRNA was assessed in control (WT, ROSA and Mck-Cre [14]) and

m-V59M mice using semi-quantitative PCR (Fig. 1a). To distinguish between WT and mutant mRNA we exploited the fact that introduction of the V59M mutation removes a unique BtsCI restriction site in the *Kcnj11* cDNA. Thus, the presence of two bands on the gel indicates WT *Kcnj11* mRNA alone whereas three bands indicates the presence of both WT and mutant (V59M) *Kcnj11* mRNAs. Figure 1a confirms that mRNA encoding Kir6.2-V59M is expressed in the heart and skeletal muscle, but not the brain, of m-V59M mice. As expected mutant mRNA is not expressed in control (WT, ROSA and Mck-Cre) mice.

To determine the relative amount of *Kcnj11* and *Abcc9* expression in control and m-V59M mice we performed quantitative PCR. Expression of *Kcnj11*, *Abcc9* and *Gfp* (encoding green fluorescent protein) mRNAs was expressed relative to a panel of housekeeping genes (*Actb*, *Hprt1* and *Hspa8*). Figure 1b shows that there was no change in *Kcnj11* mRNA expression in brain of m-V59M mice, but that *Kcnj11* expression was increased by about 90% in hearts of m-V59M mice compared with controls. This increase can be attributed to mRNA encoding Kir6.2-V59M, as shown from the level of expression of *Gfp* (Fig. 1c), which lies downstream of the mutated *Kcnj11* gene and is transcribed from the same promoter. This indicates that there is roughly the same amount of WT and mutant *Kcnj11* mRNAs. Thus, at the RNA level this establishes the hemizygous m-V59M mouse as a plausible model for human patients with iDEND syndrome, all of who are heterozygotes [2, 3].

Despite the increase in total *Kcnj11* mRNA, the overall K_{ATP} channel density should remain relatively constant as *Abcc9* mRNA expression was unchanged in the heart (Fig. 1d), and Kir6.2 is unable to traffic to the membrane in the absence of SUR [38].

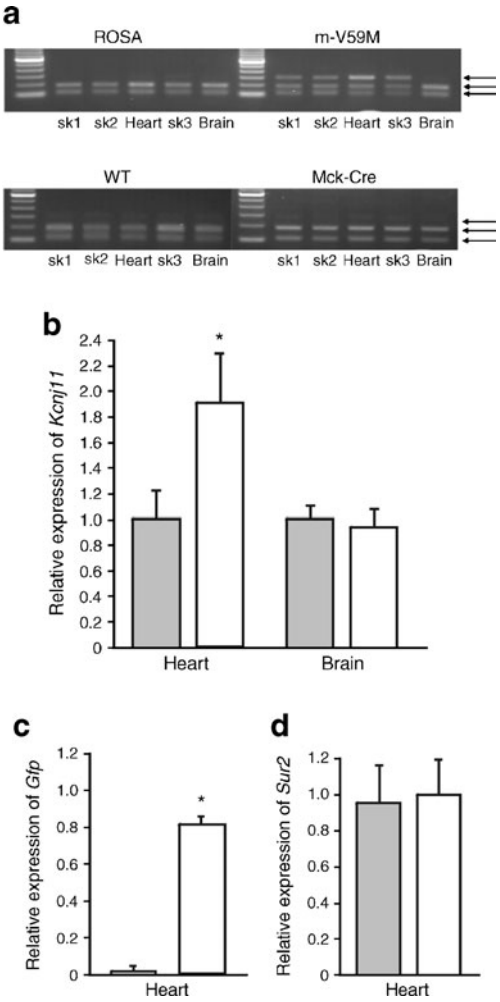

Fig. 1 *Kcnj11* expression in the heart. **a** *Kcnj11* expression in tissue isolated from ROSA, WT, Mck-Cre and m-V59M mice. WT, but not mutant (V59M), *Kcnj11* cDNA is cut by the restriction enzyme BtsCI: the presence of two bands thus indicates the presence of the WT gene only and three bands indicates both WT and mutant genes. Data are representative of experiments on seven ROSA, four m-V59M, four WT and four Mck-Cre mice. sk1, quadriceps muscle; sk2, triceps muscle; sk3, diaphragm. **b,c** Quantitative PCR showing expression of *Kcnj11* in heart and brain (**b**) and *Gfp* in heart (**c**) of control (grey bars, $n=5$) and m-V59M mice (white bars, $n=5$), relative to a panel of housekeeping genes. $^{*}p<0.05$ against controls. **d** Quantitative PCR showing expression of *Abcc9* in heart of control (grey bars, $n=5$) and m-V59M mice (white bars, $n=5$), relative to a panel of housekeeping genes. No significant differences were seen

ATP sensitivity of K_{ATP} channels in V59M heart

Patch-clamp recordings of isolated ventricular myocytes from m-V59M mice revealed that the magnitude of the K_{ATP} current recorded in inside-out patches in the absence of nucleotides was not significantly different in WT and mutant myocytes, being 287±75 pA ($n=14$) and 453±99 pA ($n=14$) respectively ($p\sim0.2$). No currents were detected in cell-attached patches on either WT or mutant myocytes.

The ATP sensitivity of the native muscle K_{ATP} channel was significantly reduced compared with control mice (Fig. 2a-d). The half-maximal inhibitory concentration (IC_{50}) shifted from 13±1 μmol/l ($n=14$ patches, four mice) for WT channels to 62±7 μmol/l ($n=10$ patches, $n=3$ mice) for channels recorded from m-V59M myocytes (Fig. 2e). This indicates that the mutant protein is present in the heart. The concentration–inhibition relationship was best fitted with a single Hill equation.

Cardiac MRI

Cardiac MRI was performed on 12-week-old control and m-V59M mice (Fig. 3a–c). Body weight and resting heart rates under anaesthesia were similar between control and m-V59M mice (Fig. 4a, Table 1). In vivo measurements of left ventricular (LV) ejection fractions, volumes and cardiac outputs identified no differences between groups (Fig. 4b–c, Table 1). Left ventricular mass and septal wall thickness were also similar in control and m-V59M mice (Fig. 4f, Table 1).

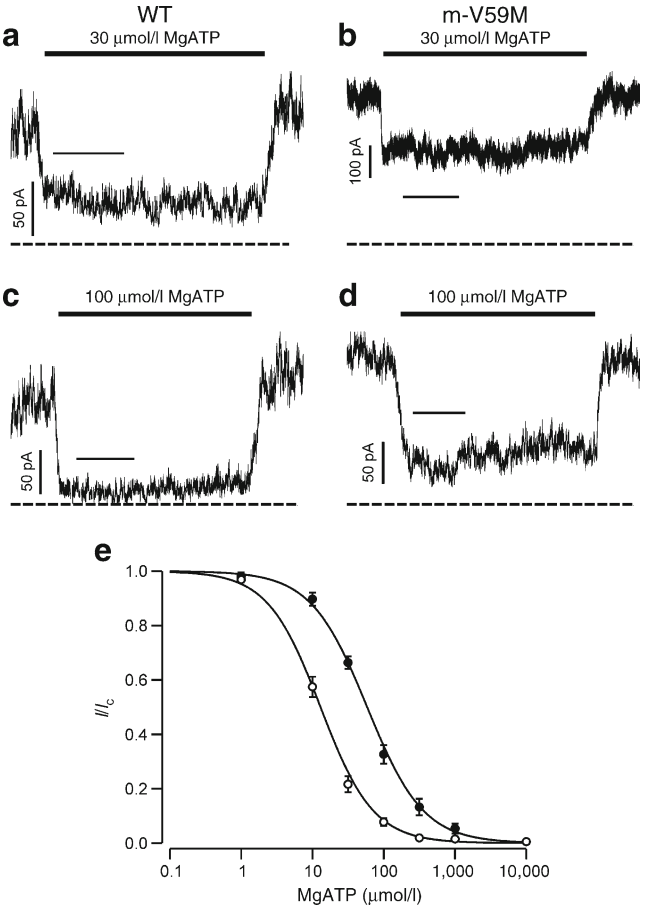

Fig. 2 ATP sensitivity of cardiac K_{ATP} channels in control and m-V59M mice. **a–d** K_{ATP} channel currents recorded at −60 mV in inside-out patches from control (**a**,**c**) or m-V59M (**b**,**d**) cardiac myocytes. The solid bar indicates application of 30 μmol/l or 100 μmol/l MgATP, as indicated. The dashed line indicates the zero current potential. Horizontal bars indicate 5 s. **e** Mean relationship between MgATP concentration and K_{ATP} current (I), expressed relative to that in the absence of nucleotide (I_c), for WT (white circles, n=14 patches, four mice) and m-V59M (black circles, n=10 patches, three mice) channels. The lines are drawn to equation 1, with the following parameters: WT (IC_{50}= 13 μmol/l, h=1.2); m-V59M (IC_{50}=59 μmol/l, h=1.1)

We next carried out stress tests on cardiac function. Intraperitoneal administration of 1.5 mg/kg dobutamine resulted in a significant elevation in heart rate within 5 min of injection (Figs 3 and 4d, Table 2). Dobutamine increased LV ejection fractions and cardiac outputs, and reduced end diastolic and end systolic volumes (Fig. 4a–e, Table 2). It also increased end diastolic and end systolic septal wall thickness (Fig. 4f). Similar responses to dobutamine stress were observed in control and m-V59M mice (Fig. 4, Table 2).

Discussion

Our results suggest that m-V59M mice have normal hearts. There were no gross morphological differences observed between images of m-V59M and control hearts, and no differences in a variety of measures of cardiac function under resting conditions, including heart rates, LV ejection fractions, end diastolic, end systolic and stroke volumes, cardiac outputs, mass and wall thickness. In response to dobutamine stress, heart rates, ejection fractions, cardiac outputs and wall thickness increased, while end diastolic and end systolic volumes decreased, as expected, but there were still no differences between the two sets of mice. Thus, we conclude that expression of the Kir6.2-V59M subunit in the heart had no marked effect on heart function, even under stress conditions. This is in marked contrast to knockout of Kir6.2, which reduces the capacity to cope with cardiac stress [24, 25].

A similar effect was found in a different K_{ATP} channel gain-of-function mouse model [31]. Although this mutation produced a 40-fold reduction in the ATP sensitivity of the cardiac K_{ATP} channel, these mice had normal electrocardiograms and their hearts showed no gross physiological or morphological problems. In contrast to our mice, however, ΔN30,K185Q mice showed an impaired response to β-adrenergic receptor stimulation [32]. This difference may be because Rajashree and colleagues used isolated perfused hearts and isoproterenol infusion, while we injected a bolus of dobutamine into the living animal and measured in vivo cardiac function using MRI. The isolated hearts beat at a much lower intrinsic rate than in the whole animal, presumably due to loss of sympathetic innervation and circulating hormones: this likely explains why the heart rates of both control and mutant mice in our experiments were similar to those of Rajashree and colleagues in the presence of β-adrenergic agonists, but were faster under resting conditions [32]. Studies of action potential duration and cardiac function in isolated hearts from m-V59M mice would help address whether this idea is correct and, potentially, might identify differences in cardiac function between m-V59M and control mice. Nevertheless, the lack of in vivo differences suggests that in vitro experiments would yield the same result.

Electrophysiological studies showed that the IC_{50} for ATP inhibition of K_{ATP} channels in ventricular myocytes isolated from m-V59M mice (62 μmol/l) is similar to that found for skeletal muscle (67±11 μmol/l) [16] and for Kir6.2-V59M/SUR2A channels heterologously expressed in *Xenopus* oocytes (79±18 μmol/l). This provides evidence that the Kir6.2-V59M subunit is present at the protein level and indicates that the m-V59M mouse provides a valid model for the heterozygous state of patients carrying the Kir6.2-V59M mutation.

The lack of an obvious effect of the Kir6.2-V59M mutation on cardiac function resembles that found for skeletal muscle [16]. In both tissues, the mutant subunits are expressed in approximately equal amounts to WT subunits and form K_{ATP} channels with reduced ATP sensitivity—yet

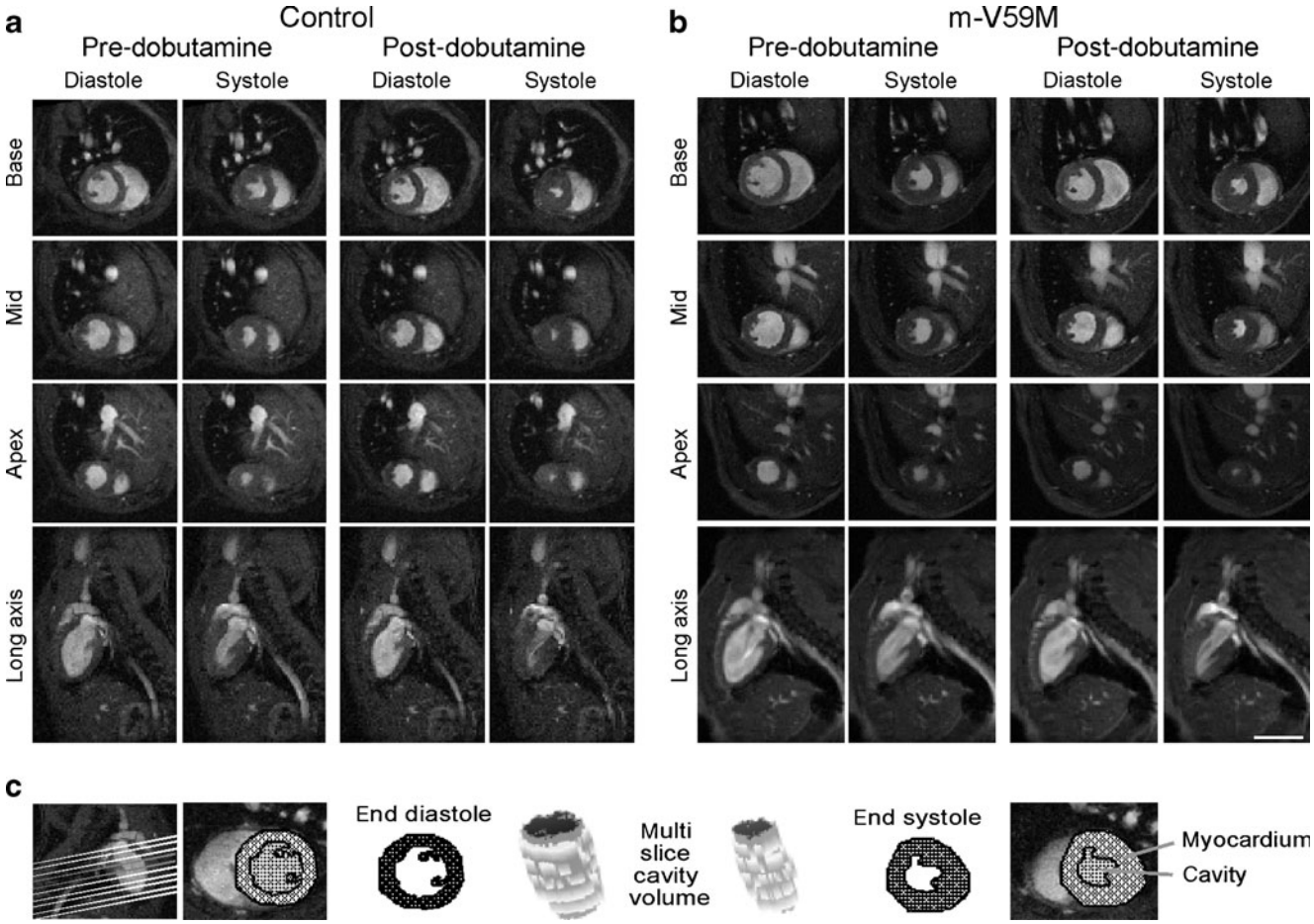

Fig. 3 Cardiac MRI of control and m-V59M mice. In vivo MRI on 12-week-old control and m-V59M mice. Typical in vivo cine-MRI images acquired in short-axis (base, mid-LV and apex) and long-axis (two-chamber) views at end diastole and end systole prior to and after administration of dobutamine. Morphology and function of the control mouse heart (**a**) were similar to the m-V59M mouse heart (**b**). Scale bar, 5 mm. **c** The multi-slice segmentation method for calculation of LV myocardial mass and cavity volume at end diastole and end systole

muscle function appears unaffected. In contrast, the presence of Kir6.2-V59M in nerve or pancreatic beta cells has profound functional effects [14, 16]. This difference may be a consequence of the different SUR subunits that comprise the cardiac/skeletal muscle (Kir6.2/SUR2A) and the beta cell/brain K_{ATP} channels (Kir6.2/SUR1). As discussed above, different subtypes of cardiac myocyte have different types of SUR subunit, with SUR1 being the prevalent subtype in atrial cells and SUR2A in ventricular cells [29]. Our experiments primarily measure ventricular function (Kir6.2/SUR2A subunits). Similarly, although a significant amount of SUR1 mRNA was found in fast twitch muscle, SUR2A is the most abundant subunit expressed in all skeletal muscle fibre types tested [39].

The origin of the different metabolic sensitivities of Kir6.2/SUR2A and KirR6.2/SUR1 channels is unclear. When heterologously expressed in *Xenopus* oocytes, Kir6.2-V59M/SUR1 channels are opened by metabolic inhibition whereas Kir6.2-V59M/SUR2A channels are not [16]. Precisely why this is the case is still not clear. However, while ATP block and MgADP activation are not different for the two types of channel, MgADP can reduce ATP inhibition of Kir6.2-V59M/SUR1 channels but not Kir6.2-V59M/SUR2A channels [16]. This suggests that the molecular basis of differential metabolic sensitivity of SUR1 and SUR2A channels is due to altered nucleotide handling by the different sulfonylurea receptors.

There is good evidence that atrial K_{ATP} channels are composed of Kir6.2/SUR1 channels [20], which show a greater metabolic sensitivity than Kir6.2/SUR2A channels. Thus we might have expected an effect of the Kir6.2-V59M mutation on atrial function. As this was not seen, it suggests that atrial K_{ATP} channels are largely closed in the resting and stressed states and that their activation by the Kir6.2-V59M mutation is not sufficient to affect ventricular function. We did not measure atrial function directly. Nevertheless, we did not identify changes in atrial size on long-axis MR scout images, and it is likely that gross changes in atrial function would have led to secondary changes in ventricular function, which we did not observe. In the future it would be interesting to perform additional studies to look at atrial function directly.

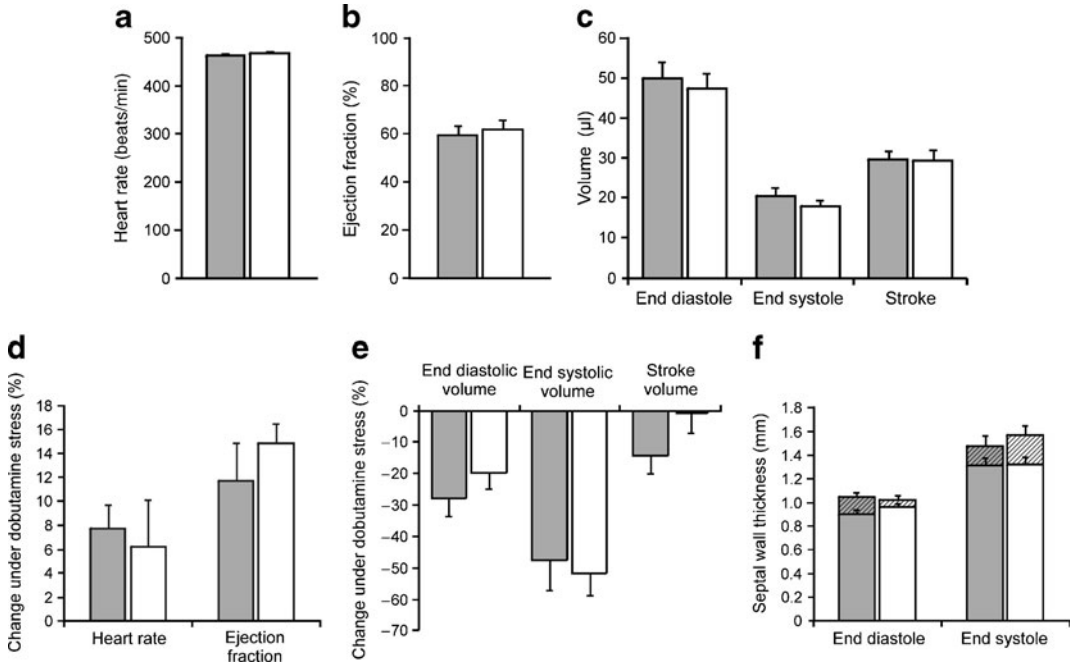

Fig. 4 Cardiac function and morphology in control and m-V59M mice. Heart rate (**a**), ejection fraction (**b**) and end diastolic, end systolic and stroke volume (**c**) were similar in control (grey bars, $n=6$) and m-V59M (white bars, $n=5$) mouse hearts. Heart rate and ejection fraction (**d**) increased, while end diastolic and end systolic volume (**e**) decreased under dobutamine stress. The response to dobutamine stress was similar in control (grey bars, $n=6$) and m-V59M (white bars, $n=5$) mouse hearts. **f** At rest there was no difference in septal wall thickness between control and m-V59M mice (lower bars). Dobutamine increased end diastolic and end systolic septal wall thickness (upper bars), $p<0.05$. A similar response to dobutamine was observed in control (grey bars, $n=6$) and m-V59M (white bars, $n=5$) mice

To date, none of the mutations in the *KCNJ11* (Kir6.2) and *ABCC8* (SUR1) genes that cause neonatal diabetes in human patients have been linked to cardiac dysfunction [2, 3, 6]. It is important to be cautious when extrapolating from mouse models to humans, especially in the case of the heart (the mouse heart rate is far higher). Nevertheless, the detailed study reported here suggests that this is probably because gain-of-function K_{ATP} channel mutations do not cause cardiac abnormalities, rather than heart problems existing, but being undetected. They also suggest that patients are unlikely to develop cardiac problems when adrenaline (epinephrine) levels rise (during exercise or in stressful states) as a consequence of the expression of a gain-of-function K_{ATP} channel in the heart. However, it remains possible that impaired cardiac function may be exacerbated under ischaemic

Table 1 Cardiac morphology and function assessed by MRI

Variable	Control ($n=6$)	m-V59M ($n=5$)
Heart rate (beats/min)	464±23	468±65
Ejection fraction (%)	60±2	62±1
End diastolic volume (μl)	50±4	47±4
End systolic volume (μl)	20±2	18±2
Stroke volume (μl)	30±2	29±3
Cardiac output (ml/min)	14±1	14±2
LV mass (mg)	73±6	73±4
Body weight (g)	25±2	26±2

Data are means±SEM for 12-week-old control ($n=6$) and m-V59M ($n=5$) mice

Data were analysed using a Student's *t* test; no significant differences between control and mV59M mice were identified

Table 2 Changes in cardiac function under dobutamine stress assessed by MRI

Variable	Change under dobutamine stress (%)	
	Control ($n=6$)	m-V59M ($n=5$)
Heart rate	8±2*	6±4*
Ejection fraction	12±3***	15±2***
End diastolic volume	−28±6**	−20±5**
End systolic volume	−48±9***	−52±7***
Stroke volume	−14±6	−1±6
Cardiac output	8±2*	5±2*

Data are means±SEM for 12-week-old control ($n=6$) and m-V59M ($n=5$) mice

Data were compared with those acquired before stress using a repeated-measures ANOVA (with genotype as a between-subject factor and dobutamine treatment as a within-subject factor)

* $p<0.05$, ** $p<0.01$ and *** $p<0.001$ against pre-dobutamine data; there were no significant differences between control and m-V59M mice

conditions or could arise in patients with neonatal diabetes as a secondary consequence of poor control of glucose homeostasis. Studies of ischaemia–reperfusion in vivo and in isolated hearts from m-V59M mice might be valuable in this respect.

Finally, sulfonylureas are now first-line therapy for neonatal diabetes, with glibenclamide being the usual choice [40]. The choice of sulfonylurea used for type 2 diabetes therapy has long been debated [41–43]. In particular, there has been concern that some drugs, such as glibenclamide, may interact adversely with cardiac (SUR2A-containing) K_{ATP} channels. K_{ATP} channel activation plays an important role in cardiac ischaemic preconditioning [7, 9], and this effect is prevented by glibenclamide [44]. Patients with neonatal diabetes routinely require much higher sulfonylurea doses than patients with type 2 diabetes and may be expected to take the drugs for far longer. Our demonstration that cardiac function is unimpaired in m-V59M mice argues that mutant cardiac K_{ATP} channels remain closed and thus it may not be necessary to use a sulfonylurea drug that cross-reacts with cardiac K_{ATP} channels to treat the patient's diabetes. This might be beneficial, as it would allow opening of cardiac K_{ATP} channels during ischaemia and enable ischaemic preconditioning.

Acknowledgements We thank J. Brüning, Institute of Genetics, Cologne for the gift of Mck-Cre mice. We thank K. Shimomura for dissecting the hearts and C. Bollensdorff for advice on cardiac myocyte isolation.

Funding This work was supported by the Wellcome Trust [076436/Z/05/Z, 081188/A/06/Z]; the Royal Society; the European Union [EuroDia-(LSHM-CT-2006-518153)] and the British Heart Foundation [RG/07/004/22659, RG/07/059/23259]. F. M. Ashcroft is a Royal Society Research Professor. R. Clark held a Wellcome Trust OXION PhD studentship.

Contribution statement RC and DS performed and analysed the MRI experiments and RM the patch-clamp experiments. All authors contributed to the design of the experiments and the writing of the paper. All the authors approved the final version of the paper to be published.

Duality of interest The authors declare that there is no duality of interest associated with this manuscript.

References

1. Proks P, Antcliff JF, Lippiat J, Gloyn AL, Hattersley AT, Ashcroft FM (2004) Molecular basis of Kir6.2 mutations associated with neonatal diabetes or neonatal diabetes plus neurological features. Proc Natl Acad Sci USA 101:17539–17544
2. Gloyn AL, Pearson ER, Antcliff JF et al (2004) Activating mutations in the gene encoding the ATP-sensitive potassium-channel subunit Kir6.2 and permanent neonatal diabetes. N Engl J Med 350:1838–1849
3. Hattersley AT, Ashcroft FM (2005) Activating mutations in Kir6.2 and neonatal diabetes: new clinical syndromes, new scientific insights, and new therapy. Diabetes 54:2503–2513
4. Babenko AP, Polak M, Cave H et al (2006) Activating mutations in the *ABCC8* gene in neonatal diabetes mellitus. N Engl J Med 355:456–466
5. Ashcroft FM (2007) The Walter B. Cannon Physiology in Perspective Lecture, 2007. ATP-sensitive K+ channels and disease: from molecule to malady. Am J Physiol Endocrinol Metab 293: E880–889
6. McTaggart JS, Clark RH, Ashcroft FM (2010) The role of the K_{ATP} channel in glucose homeostasis in health and disease: more than meets the islet. J Physiol 588:3201–3209
7. Flagg TP, Enkvetchakul D, Koster JC, Nichols CG (2010) Muscle K_{ATP} channels: recent insights to energy sensing and myoprotection. Physiol Rev 90:799–829
8. Miki T, Seino S (2005) Roles of K_{ATP} channels as metabolic sensors in acute metabolic changes. J Mol Cell Cardiol 38:917–925
9. Nichols CG (2006) K_{ATP} channels as molecular sensors of cellular metabolism. Nature 440:470–476
10. Tucker SJ, Gribble FM, Zhao C, Trapp S, Ashcroft FM (1997) Truncation of Kir6.2 produces ATP-sensitive K-channels in the absence of the sulphonylurea receptor. Nature 387:179–183
11. Gribble FM, Tucker SJ, Ashcroft FM (1997) The essential role of the Walker A motifs of SUR1 in K_{ATP} channel activation by MgADP and diazoxide. EMBO J 16:1145–1152
12. Shyng S, Ferrigni T, Nichols CG (1997) Regulation of K_{ATP} channel activity by diazoxide and MgADP. Distinct functions of the two nucleotide-binding folds of the sulfonylurea receptor. J Gen Physiol 110:643–654
13. Ashcroft FM, Harrison DE, Ashcroft SJ (1984) Glucose induces closure of single potassium channels in isolated rat pancreatic beta-cells. Nature 312:446–448
14. Girard CA, Wunderlich FT, Shimomura K et al (2009) Expression of an activating mutation in the gene encoding the K_{ATP} channel subunit Kir6.2 in mouse pancreatic beta cells recapitulates neonatal diabetes. J Clin Invest 119:80–90
15. Koster JC, Marshall BA, Ensor N, Corbett JA, Nichols CG (2000) Targeted overactivity of beta cell K_{ATP} channels induces profound neonatal diabetes. Cell 100:645–654
16. Clark RH, McTaggart JS, Webster R et al (2010) Muscle dysfunction caused by a K_{ATP} channel mutation in neonatal diabetes is neuronal in origin. Science 329:458–461
17. Babenko AP, Gonzalez G, Aguilar-Bryan L, Bryan J (1998) Reconstituted human cardiac K_{ATP} channels: functional identity with the native channels from the sarcolemma of human ventricular cells. Circ Res 83:1132–1143
18. Chutkow WA, Samuel V, Hansen PA et al (2001) Disruption of Sur2-containing K_{ATP} channels enhances insulin-stimulated glucose uptake in skeletal muscle. Proc Natl Acad Sci USA 98:11760–11764
19. Suzuki M, Li RA, Miki T et al (2001) Functional roles of cardiac and vascular ATP-sensitive potassium channels clarified by Kir6.2-knockout mice. Circ Res 88:570–577
20. Flagg TP, Kurata HT, Masia R et al (2008) Differential structure of atrial and ventricular K_{ATP}: atrial K_{ATP} channels require SUR1. Circ Res 103:1458–1465
21. Noma A (1983) ATP-regulated K^+ channels in cardiac muscle. Nature 305:147–148

22. Lederer WJ, Nichols CG, Smith GL (1989) The mechanism of early contractile failure of isolated rat ventricular myocytes subjected to complete metabolic inhibition. J Physiol 413:329–349
23. Suzuki M, Sasaki N, Miki T et al (2002) Role of sarcolemmal K_{ATP} channels in cardioprotection against ischemia/reperfusion injury in mice. J Clin Invest 109:509–516
24. Tong X, Porter LM, Liu G et al (2006) Consequences of cardiac myocyte-specific ablation of K_{ATP} channels in transgenic mice expressing dominant negative Kir6 subunits. Am J Physiol Heart Circ Physiol 291:H543–551
25. Zingman LV, Hodgson DM, Bast PH et al (2002) Kir6.2 is required for adaptation to stress. Proc Natl Acad Sci U S A 99:13278–13283
26. Kane GC, Behfar A, Yamada S et al (2004) ATP-sensitive K^+ channel knockout compromises the metabolic benefit of exercise training, resulting in cardiac deficits. Diabetes 53:S169–175
27. Kane GC, Behfar A, Dyer RB et al (2006) *KCNJ11* gene knockout of the Kir6.2 K_{ATP} channel causes maladaptive remodeling and heart failure in hypertension. Hum Mol Genet 15:2285–2297
28. Yamada S, Kane GC, Behfar A et al (2006) Protection conferred by myocardial ATP-sensitive K^+ channels in pressure overload-induced congestive heart failure revealed in *KCNJ11* Kir6.2-null mutant. J Physiol 577:1053–1065
29. Fedorov VV, Glukhov AV, Ambrosi CM (2011) Effects of K_{ATP} channel openers diazoxide and pinacidil in coronary-perfused atria and ventricles from failing and non-failing human hearts. J Mol Cell Cardiol 51:215–25
30. Flagg TP, Charpentier F, Manning-Fox J et al (2004) Remodeling of excitation-contraction coupling in transgenic mice expressing ATP-insensitive sarcolemmal K_{ATP} channels. Am J Physiol Heart Circ Physiol 286:H1361–1369
31. Koster JC, Knopp A, Flagg TP et al (2001) Tolerance for ATP-insensitive K_{ATP} channels in transgenic mice. Circ Res 89:1022–1029
32. Rajashree R, Koster JC, Markova KP, Nichols CG, Hofmann PA (2002) Contractility and ischemic response of hearts from transgenic mice with altered sarcolemmal K_{ATP} channels. Am J Physiol Heart Circ Physiol 283:H584–590
33. Bruning JC, Michael MD, Winnay JN et al (1998) A muscle-specific insulin receptor knockout exhibits features of the metabolic syndrome of NIDDM without altering glucose tolerance. Mol Cell 2:559–569
34. Stuckey DJ, Carr CA, Tyler DJ, Aasum E, Clarke K (2008) Novel MRI method to detect altered left ventricular ejection and filling patterns in rodent models of disease. Magn Reson Med 60:582–587
35. Stuckey DJ, Carr CA, Tyler DJ, Clarke K (2008) Cine-MRI versus two-dimensional echocardiography to measure in vivo left ventricular function in rat heart. NMR Biomed 21:765–772
36. Tyler DJ, Lygate CA, Schneider JE, Cassidy PJ, Neubauer S, Clarke K (2006) CINE-MR imaging of the normal and infarcted rat heart using an 11.7 T vertical bore MR system. J Cardiovasc Magn Reson 8:327–333
37. Song W, Dyer E, Stuckey D et al (2010) Investigation of a transgenic mouse model of familial dilated cardiomyopathy. J Mol Cell Cardiol 49:380–389
38. Zerangue N, Schwappach B, Jan YN, Jan LY (1999) A new ER trafficking signal regulates the subunit stoichiometry of plasma membrane K_{ATP} channels. Neuron 22:537–548
39. Tricarico D, Mele A, Lundquist AL, Desai RR, George AL Jr, Conte Camerino D (2006) Hybrid assemblies of ATP-sensitive K^+ channels determine their muscle-type-dependent biophysical and pharmacological properties. Proc Natl Acad Sci U S A 103:1118–1123
40. Pearson ER, Flechtner I, Njolstad PR et al (2006) Switching from insulin to oral sulfonylureas in patients with diabetes due to Kir6.2 mutations. N Engl J Med 355:467–477
41. Quast U, Stephan D, Bieger S, Russ U (2004) The impact of ATP-sensitive K^+ channel subtype selectivity of insulin secretagogues for the coronary vasculature and the myocardium. Diabetes 53: S156–164
42. Simpson SH, Majumdar SR, Tsuyuki RT, Eurich DT, Johnson JA (2006) Dose-response relation between sulfonylurea drugs and mortality in type 2 diabetes mellitus: a population-based cohort study. CMAJ 174:169–174
43. UKPDS-group (1998) Intensive blood-glucose control with sulphonylureas or insulin compared with conventional treatment and risk of complications in patients with type 2 diabetes (UKPDS 33). UK Prospective Diabetes Study (UKPDS) Group. Lancet 352:837–853
44. Ghosh S, Standen NB, Galinianes M (2001) Failure to precondition pathological human myocardium. J Am Coll Cardiol 37:711–718